

Cell Cycle Regulation of Myosin-V by Calcium/Calmodulin-Dependent Protein Kinase II

Ryan L. Karcher,¹ Joseph T. Roland,¹ Francesca Zappacosta,² Michael J. Huddleston,² Roland S. Annan,² Steven A. Carr,^{2*} Vladimir I. Gelfand^{1†}

Organelle transport by myosin-V is down-regulated during mitosis, presumably by myosin-V phosphorylation. We used mass spectrometry phosphopeptide mapping to show that the tail of myosin-V was phosphorylated in mitotic *Xenopus* egg extract on a single serine residue localized in the carboxyl-terminal organelle-binding domain. Phosphorylation resulted in the release of the motor from the organelle. The phosphorylation site matched the consensus sequence of calcium/calmodulin-dependent protein kinase II (CaMKII), and inhibitors of CaMKII prevented myosin-V release. The modulation of cargo binding by phosphorylation is likely to represent a general mechanism regulating organelle transport by myosin-V.

The partitioning and transport of organelles in eukaryotic cells is achieved by the regulated action of motor proteins that bind to organelles and transport them along microtubules and actin filaments to ensure proper localization in the cell. During mitosis, movement of cytoplasmic organelles usually ceases, preventing the interference of organelles with components of the cell-division machinery and ensuring stochastic partitioning of multicopy organelles between daughter cells (1). *Xenopus* melanophores provide a convenient system to study the regulation of organelle transport. The concerted efforts of two microtubule motors, kinesin-II and cytoplasmic dynein, and an actin motor, myosin-V, achieve movement of pigment organelles (melanosomes) in melanophores (2–4). Because melanosomes do not respond to hormonal signals during mitosis, activity of these motors may be down-regulated during cell division (5). Whereas the regulation of microtubule motors in the cell cycle has been documented in other cell types (6, 7), the melanophore system can be used for analysis of the regulation of myosin-based organelle transport. Myosin-V-driven transport of melanosomes is inhibited by their incubation in mitotic, but not interphase, *Xenopus* egg extract because of the dissociation of the

motor from the surface of melanosomes (8). Myosin-V could be regulated in the cell cycle through the modification of its COOH-terminal tail domain, a part of the motor that is involved in cargo binding (9, 10).

To test whether the COOH-terminal globular domain of myosin-V tail (MGT) was sufficient for melanosome binding, we transfected melanophores with a construct encoding myc epitope-tagged MGT (amino acids 1443 to 1853 of mouse dilute myosin-Va) in the plasmid pcDNA3 (11). Melanosomes from transfected cultures were purified and probed for bound myc-MGT. Myc-MGT indeed bound to melanosomes (Fig. 1A). To determine whether the binding of myc-MGT was cell cycle-regulated in the same way as the binding of the endogenous motor, we treated melanosomes from transfected cultures with *Xenopus* egg extracts as previously described (8). Both endogenous, full-length myosin-V and mouse myc-MGT were released from melanosomes after treatment with mitotic but not with interphase extract (Fig. 1, A and B). Thus, myosin-V release was determined by the modification of its COOH-terminal globular domain and did not require the presence of other parts of the molecule. In addition, mouse MGT accurately reproduced the behavior of endogenous, full-length myosin-V from *Xenopus* and could be used to study myosin-V regulation.

The release of myosin-V from melanosomes by mitotic extract correlates with its phosphorylation (8); therefore, MGT should contain the phosphorylation site. To test this hypothesis, we expressed MGT in *Escherichia coli* as a fusion protein with glutathione S-transferase (GST). The recombinant protein

was bound to glutathione-agarose beads (12); beads with fusion protein were incubated in extracts supplemented with [γ -³²P]adenosine 5'-triphosphate (ATP) (13). After incubation, MGT was cleaved from GST with thrombin and analyzed by SDS-polyacrylamide gel electrophoresis (PAGE) and autoradiography. MGT was heavily phosphorylated in mitotic but not interphase extracts (Fig. 2A). Thus, the phosphorylation of myosin-V tail likely induced its dissociation from organelles.

We used recombinant MGT phosphorylated by mitotic extracts to map the site of phosphorylation with a multidimensional mass spectrometry-based strategy (14). Tryptic digests of MGT treated with mitotic and interphase egg extracts were analyzed for phosphopeptide content by online liquid chromatography-electrospray mass spectrometry, monitoring for the highly diagnostic phosphopeptide marker ion mass-to-charge ratio (m/z) 79 (PO_3^-) (15). A comparison of the marker ion trace for the mitotic and interphase MGT samples (Fig. 2B) showed an increase in the level of phosphorylation present in a cluster of three chromatographic peaks (labeled 7 to 9 in Fig. 2B). We used matrix-assisted laser desorption/ionization-post source decay (MALDI-PSD) (16) to show that these peaks contained a phosphopeptide of mass 1920.9 daltons, which corresponded to an MGT tryptic peptide, TSSIADEGTYTLDSILR (17), plus 1 mol of phosphate. To define the location of the modified residue from among the seven potential phosphorylation sites, we sequenced the 1920.9-dalton peptide in each of the three fractions (18) using nanoelectrospray tandem mass spectrometry (MS/MS). Sequence data from all three fractions showed that the phosphorylation site is located within the first three residues of each peptide (corresponding to Thr¹⁶⁴⁸, Ser¹⁶⁴⁹, and Ser¹⁶⁵⁰ in full-length mouse myosin-Va); however, we were unable to assign the specific site of modification for any of them. The MS/MS spectrum of the peptide from the most abundant fraction (fraction 8) contained some evidence to suggest that the major site of phosphorylation is Ser¹⁶⁵⁰ (Fig. 2C). To rule out the possibility that we had overlooked additional phosphorylated sequences in fractions 7 to 9, we combined the fractions and analyzed them by nanoelectrospray MS with a precursor ion scan of m/z 79 (18). No other sequences were detected, which confirmed that a single peptide was selectively phosphorylated in mitotic extracts.

To unambiguously localize the site(s) of phosphorylation, we generated seven mutant versions of MGT with all possible single, double, and triple substitutions of serine and threonine in positions 1648 to 1650 to alanine, and we compared the phosphorylation of mutant and wild-type proteins in mitotic

¹Department of Cell and Structural Biology, University of Illinois at Urbana-Champaign, Urbana, IL 61801, USA. ²Department of Physical and Structural Chemistry, GlaxoSmithKline, King of Prussia, PA 19406, USA.

*Present address: Millennium Pharmaceuticals, Cambridge, MA 02139, USA.

†To whom correspondence should be addressed. E-mail: vgelfand@life.uiuc.edu

REPORTS

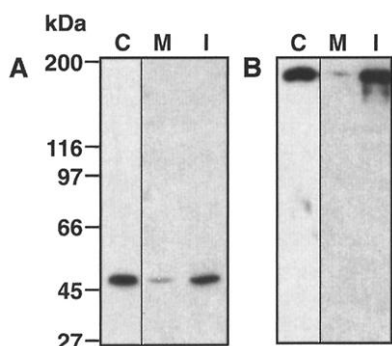


Fig. 1. Mouse MGT binds to *Xenopus* melanosomes and dissociates in mitotic egg extract. (A) MGT is dissociated from melanosomes in mitotic extract. Western blotting was done with the antibody to myc 1-9E10.2. MGT bound to melanosomes (C) and was retained after treatment with interphase egg extract (I) but was released after treatment with mitotic extract (M). (B) Myosin-V is dissociated from melanosomes in mitotic extract. Western blotting was done with polyclonal antibody DIL-2 against myosin-V (8). Melanosomes (C), melanosomes treated with mitotic egg extract (M), and melanosomes treated with interphase egg extract (I) are shown.

extracts (11). Only the mutation in position 1650 affected phosphorylation (Fig. 2D). Hence, a protein kinase(s) in mitotic extract selectively phosphorylated MGT at Ser¹⁶⁵⁰.

Mapping of the mitotic phosphorylation site allowed us to test whether phosphorylation indeed releases myosin-V from melanosomes. If phosphorylation regulates binding, the substitution in MGT (MGT-Ser1650Ala) should create a protein that binds to melanosomes but cannot be phosphorylated and released by mitotic extracts. On the other hand, replacement with negatively charged glutamic acid should mimic the phosphorylated state, and MGT carrying this substitution should be unable to bind to melanosomes.

Constructs encoding the mutant or wild-type forms of myc-MGT were expressed in melanophores, melanosomes were purified and incubated in mitotic extracts, and binding to melanosomes and release was analyzed by Western blotting (8). The results of this experiment demonstrate that both wild-type and Ser1650Ala forms of MGT bound to melanosomes. However, unlike the wild-type protein, MGT-Ser1650Ala did not dissociate from organelles in mitotic extracts (Fig. 3A). Conversely, MGT-Ser1650Glu could not bind to melanosomes.

If the phosphorylation of myosin-V governs organelle binding, what kinase or phosphatase is responsible for this regulation? Two obvious candidates for this phosphorylation are p34(Cdc2) and Plx1, two protein kinases that are known to be up-regulated during mitosis (19, 20). Both of these kinases phosphorylate recombinant myc-MGT in vitro. However, they phosphorylate MGT-

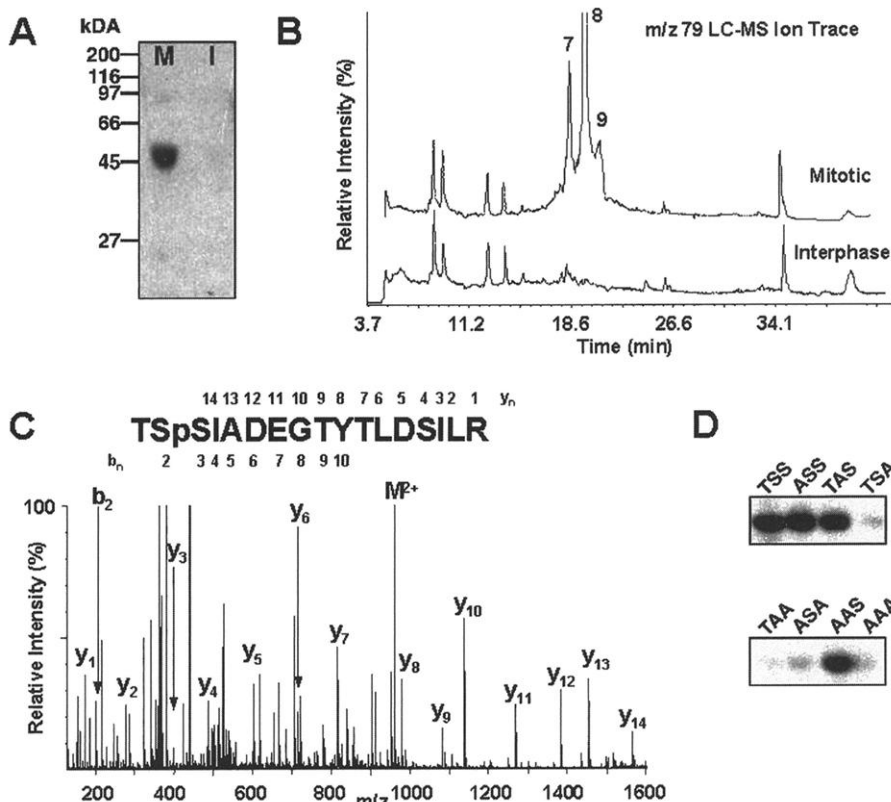


Fig. 2. Mitotic phosphorylation of Ser¹⁶⁵⁰ of myosin-V and phosphopeptide analysis. (A) Phosphorylation of recombinant MGT in *Xenopus* egg extracts. MGT purified on glutathione agarose beads (12) was phosphorylated in mitotic extract (M) but not in interphase egg extract (I). (B) Phosphopeptide-selective liquid chromatography electrospray-MS analysis (14) of MGT treated with mitotic (top) or interphase (bottom) egg extract (37). SDS-PAGE bands were excised and digested in situ with trypsin. Tryptic digests of each sample were fractionated by reverse phase HPLC. The column flow was split 10:1, with 3.6 μ l/min being collected as fractions and 0.4 μ l/min sent to the mass spectrometer, which was operated in the negative ion mode and optimized to detect the phosphate-specific marker ion, m/z 79 (PO_3^-), produced by collision-induced dissociation (CID) in the ion source of the mass spectrometer. Fractions 7 to 9 were analyzed by MALDI-PSD and were found to each contain a phosphopeptide of mass 1920.9. Under PSD conditions, phosphopeptides lose H_3PO_4 from phospho-serine and -threonine side chains and HPO_3 from phosphotyrosine side chains to produce intense-98 daltons and $[M+H]^-$ -80 daltons fragment ions. Thus, phosphopeptides can be easily distinguished from nonphosphorylated peptides, which do not fragment to produce these ions (16). (C) CID product ion spectrum of the 1920.9-dalton phosphopeptide from fraction 8. The y_n -ion series shows that residues 1651 to 1664 are not phosphorylated. A weak b_n series is present, showing a b_2 ion corresponding to unmodified Thr¹⁶⁴⁸ and Ser¹⁶⁴⁹. All subsequent b_n ions (b_3 to b_{10}) are shifted in mass by 80 daltons. For the sake of clarity, not all ions are labeled on the spectrum. The actual sequence coverage is indicated on the peptide sequence. Nomenclature is after Biemann (34). (D) Localization of the phosphorylation site by mutagenesis in positions 1648 through 1650. The Ser or Thr residues at positions 1648 through 1650 were mutated to Ala. Amino acid sequences in positions 1648 to 1650 corresponding to wild-type, single, double, or triple alanine substitutions (17) are shown above each lane.

Ser1650Ala to the same extent as wild-type MGT. Because MGT-Ser1650Ala was not phosphorylated in mitotic egg extracts, neither p34(Cdc2) nor Plx1 are likely to be involved in myosin-V regulation. On the other hand, the mitotic phosphorylation site in MGT (R-T-S-S) matches the consensus sequence for calcium/calmodulin-dependent protein kinase II (CaMKII) (R-X-X-S/T) (17, 21). CaMKII has also been known to copurify with myosin-V during biochemical fractionation and binds to its tail domain (22). Thus, CaMKII may be responsible for the phosphorylation of myosin-V and the regulation of its binding to organelles. To test this,

we first determined whether Ser¹⁶⁵⁰ was a site for CaMKII phosphorylation. Wild-type MGT was indeed phosphorylated by purified brain CaMKII, whereas the Ser¹⁶⁵⁰ \rightarrow Ala replacement abolished the phosphorylation (Fig. 3B). Therefore, Ser¹⁶⁵⁰ is the only site accessible for CaMKII in MGT. Although both Thr¹⁶⁴⁸ and Ser¹⁶⁵⁰ fit the CaMKII consensus site, only Ser¹⁶⁵⁰ was actually phosphorylated by the kinase.

Phosphorylation of the regulatory site on MGT by CaMKII strongly suggested that it may be responsible for myosin-V phosphorylation and release. We tested whether CaMKII inhibition prevented release of my-

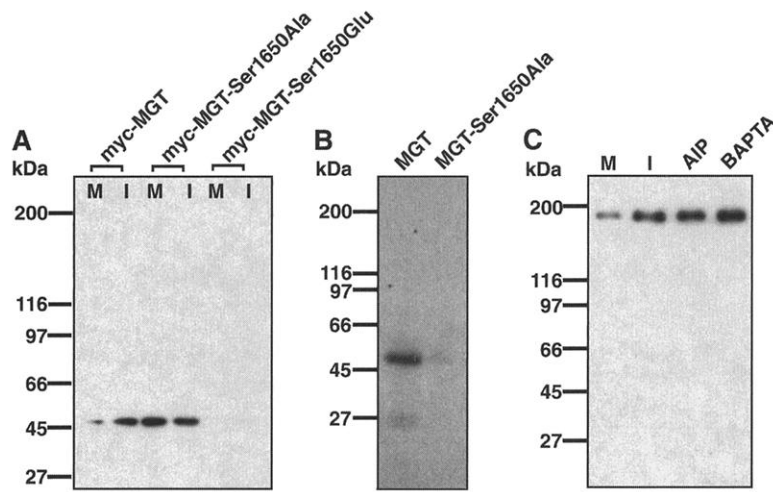


Fig. 3. Phosphorylation regulates binding and release during mitosis. **(A)** Melanosome binding of MGT, MGT-Ser1650Ala, and MGT-Ser1650Glu. Melanophores were transfected with the following constructs (35): wild-type myc-MGT, myc-MGT-Ser1650Ala, or myc-MGT-Ser1650Glu. Melanosomes were purified (36), incubated with *Xenopus* egg extracts, repurified, and subjected to Western blotting. Wild-type and mutant proteins are listed above each pair of lanes, and the treatment with either mitotic (M) or interphase (I) egg extract is listed below. **(B)** Autoradiography of an in vitro kinase assay. Purified mouse brain CaMKII phosphorylates wild-type MGT but not MGT-Ser1650Ala. **(C)** Inhibitors of CaMKII prevent the release of endogenous myosin-V from melanosomes in mitotic egg extract. As previously shown, mitotic egg extract (M) dissociated myosin-V from melanosomes, whereas interphase egg extract (I) did not. AIP (10 μ M) or 5,5'-dibromo-BAPTA (10 mM) prevented myosin-V release from the melanosome surface when added to mitotic egg extract.

osin-V by mitotic extracts. The treatment of mitotic extracts with CaMKII inhibitors, the calcium chelator 5,5'-dibromo-1,2-bis(2-aminophenoxy)ethane-*N,N,N',N'*-tetraacetic acid (BAPTA) or the highly specific peptide inhibitor autocamtide-2-related inhibitory peptide (AIP) (23), strongly inhibited release (Fig. 3C). These inhibitors did not affect HI kinase activity of mitotic extracts and therefore did not prevent release by converting mitotic extracts to an interphase state. Thus, CaMKII was responsible for the regulation of myosin-V binding to organelles. Consistent with this idea, we found that activity of CaMKII toward a specific peptide substrate (SignaTECT-CaMKII assay system, Promega, Madison, Wisconsin) in mitotic extracts is three to eight times that in interphase extracts, and that 5,5'-dibromo-BAPTA inhibited myosin-V phosphorylation in mitotic extracts. The involvement of CaMKII in the mitotic regulation of myosin-V is also consistent with the fact that its activation is required for mitotic progression in cultured cells (24) and that the level of free Ca^{2+} in frog-egg extracts is sufficient for the activation of CaMKII (25).

The phosphorylation of myosin-V tail by CaMKII regulates its binding to melanosomes in *Xenopus* melanophores, explaining cell cycle-dependent inhibition of organelle transport on actin filaments. However, we believe that tail phosphorylation may be a common mechanism regulating organelle transport by myosin-V in vertebrate cells rather than a peculiar feature of *Xenopus*

pigment cells. First, although the sequence of *Xenopus* myosin-V is not yet known, conservation of the CaMKII site described here in all three forms (a, b, and c) of myosin-V in all vertebrates suggests a universal mechanism of regulation. Second, myosin-V and CaMKII copurify in vitro (22). Third, these two proteins are often found together in vivo. For example, in neurons they are found in postsynaptic densities (26) and on synaptic vesicles (27, 28). It is possible that CaMKII regulates myosin-V functions in neurons with the same basic mechanism that is described here for pigment cells.

References and Notes

1. G. Warren, W. Wickner, *Cell* **84**, 395 (1996).
2. M. C. Tuma et al., *J. Cell Biol.* **143**, 1547 (1998).
3. H. Nilsson, M. Wallin, *Cell Motil. Cytoskel.* **38**, 397 (1997).
4. S. L. Rogers, V. I. Gelfand, *Curr. Biol.* **8**, 161 (1998).
5. S. M. Starodubov, V. A. Golichenkov, *Ontogenez* **19**, 279 (1988).
6. V. J. Allan, R. D. Vale, *J. Cell Biol.* **113**, 347 (1991).
7. J. Niclas, V. J. Allan, R. D. Vale, *J. Cell Biol.* **133**, 585 (1996).
8. S. L. Rogers et al., *J. Cell Biol.* **146**, 1265 (1999).
9. N. L. Catlett, L. S. Weisman, *Proc. Natl. Acad. Sci. U.S.A.* **95**, 14799 (1998).
10. X. Wu et al., *J. Cell Biol.* **143**, 1899 (1998).
11. DNA encoding the globular tail of mouse myosin-Va (MGT) was amplified from the construct pCMV2-FLAG-MC-ST (10) by the overlap extension polymerase chain reaction (PCR) technique (29, 30). Primers for the PCR reaction included the sequence encoding the myc-epitope tag. The PCR product was introduced into the multiple cloning site of the vector pGEX-4T-2 between the Bam HI and Xho I restriction sites. The plasmid pcDNA3-myc-MGT, which allows for eukaryotic cell expression, was created by ligation of the myc-MGT PCR product between the Bam HI

and Xho I restriction sites of pcDNA3 (Invitrogen, Carlsbad, CA). The sequences were confirmed by direct DNA sequencing.

12. The plasmid pGEX-4T-2-myc-MGT encodes the myc-epitope tag and the last 410 amino acids of mouse myosin-Va (dilute), fused to the COOH-terminus of GST. It was constructed from the vector pGEX-4T-2 (Pharmacia, Piscataway, NJ). Wild-type and mutant myc-MGT in pGEX-4T-2 were expressed in *E. coli* BL21(DE3) (Life Technologies, Grand Island, NY) and purified by the batch procedure on glutathione-agarose beads (Sigma). Bacterial pellets were resuspended in GST buffer [phosphate-buffered saline (PBS), 5 mM dithiothreitol, pH 7.0] and supplemented with 1% Triton X-100 and protease inhibitors (10 μ g/ml each chymostatin, leupeptin, and pepstatin) before lysis in a French press at 7600 kPa. Lysates were clarified by centrifugation at 16,000g for 10 min. Supernatants were applied to 1 ml of preswelled glutathione-agarose beads for 1 hour at 4°C while rotating. Beads were washed first in 10 resin volumes of lysis buffer, followed by 10 volumes of GST buffer plus 300 mM NaCl, and finally in 10 volumes of GST buffer.
13. Half a milligram of GST-myc-MGT bound to glutathione-agarose beads was labeled in 100 μ l of either mitotic or interphase *Xenopus* egg extracts supplemented with 20 μ Ci of [γ - 32 P]ATP (ICN, Costa Mesa, CA) for 30 min. Beads were then washed in GST buffer, GST buffer plus 300 mM NaCl, and then with GST buffer again. Beads were resuspended in 100 μ l of PBS, and 40 μ g of thrombin was allowed to cleave MGT from the GST for 1 hour at 37°C. After digestion, beads were pelleted in a table-top centrifuge and discarded. Then, 20 μ l of 5 \times Laemmli sample buffer was added to the supernatant, boiled for 3 min, and analyzed by SDS-PAGE and autoradiography.
14. R. S. Annan et al., *Anal. Chem.* **73**, 393 (2001).
15. M. J. Huddleston et al., *J. Am. Soc. Mass Spectrom.* **4**, 710 (1993).
16. R. S. Annan, S. A. Carr, *Anal. Chem.* **68**, 3413 (1996).
17. Single-letter abbreviations for the amino acid residues are as follows: A, Ala; C, Cys; D, Asp; E, Glu; F, Phe; G, Gly; H, His; I, Ile; K, Lys; L, Leu; M, Met; N, Asn; P, Pro; Q, Gln; R, Arg; S, Ser; T, Thr; V, Val; W, Trp; and Y, Tyr.
18. S. A. Carr, M. J. Huddleston, R. S. Annan, *Anal. Biochem.* **239**, 180 (1996).
19. E. A. Nigg, *Curr. Opin. Cell Biol.* **10**, 776 (1998).
20. R. Ohi, K. L. Gould, *Curr. Opin. Cell Biol.* **11**, 267 (1999).
21. P. J. Kennelly, E. G. Krebs, *J. Biol. Chem.* **266**, 15555 (1991).
22. M. C. Costa et al., *J. Biol. Chem.* **274**, 15811 (1999).
23. A. Ishida et al., *Biochem. Biophys. Res. Commun.* **212**, 806 (1995).
24. R. Patel et al., *J. Biol. Chem.* **274**, 7958 (1999).
25. H. D. Lindsay, M. J. Whitaker, C. C. Ford, *J. Cell Sci.* **108**, 3557 (1995).
26. R. S. Walikonis et al., *J. Neurosci.* **20**, 4069 (2000).
27. R. Prekeris, D. M. Terrian, *J. Cell Biol.* **137**, 1589 (1997).
28. F. Benfenati et al., *Nature* **359**, 417 (1992).
29. R. Higuchi, B. Krummel, R. K. Saiki, *Nucleic Acids Res.* **16**, 7351 (1988).
30. S. N. Ho et al., *Gene* **77**, 51 (1989).
31. Coomassie-blue-stained SDS-PAGE bands from mitotic and interphase MGT were excised, reduced, alkylated, and digested with trypsin in situ as described (32). Each sample was analyzed for phosphopeptide content by a modification of the multidimensional MS-based phosphopeptide mapping procedure reported in (14, 15, 33). To enhance the sensitivity of the previously reported method, we used a microcapillary PepMap C18 high-performance liquid chromatography (HPLC) column (with a 180- μ m inside diameter) flowing at 4 μ l/min and a modified PerkinElmer Sciex API III+ triple quadrupole mass spectrometer equipped with a micro-ionspray source. The HPLC flow was split post column with 0.4 μ l/min directed into the mass spectrometer and the remaining 3.6 μ l/min manually collected into chilled PCR tubes for further analysis. The MS was operated in a single ion monitoring mode for optimal sensitivity. Phosphopeptides were identified in selected fractions by MALDI-PSD analysis (16) on a Micromass ToF-

Spec SE mass spectrometer. Single-segment PSD spectra were recorded on isolated peptide $[M+H]^+$ ions. Phosphopeptides were sequenced (18) by nano-electrospray MS/MS on a Micromass Q-ToF. Precursor ion spectra for m/z 79 (14, 18) were recorded on a modified Sciex API III+ triple quadrupole mass spectrometer equipped with a nanospray source.

32. J. L. Joyal et al., *J. Biol. Chem.* **272**, 15419 (1997).
33. R. Verma et al., *Science* **278**, 455 (1997).

34. K. Biemann, *Methods Enzymol.* **193**, 886 (1990).

35. Immortalized *Xenopus* melanophores were cultured as described (36). For in vivo binding and release experiments, eight 100-mm plates of melanophores per treatment were each transfected by electroporation with 10 μ g of pcDNA3-myc-MGT or Ser¹⁶⁵⁰ mutants of this construct. Transiently transfected cells were allowed to express protein for 48 hours before harvest.

36. S. L. Rogers et al., *Proc. Natl. Acad. Sci. U.S.A.* **94**, 3720 (1997).

37. This work was supported by NIH grant GM-52111 and NSF grant MCB95-13388. We thank R. Larson and A. Murray for discussions; R. Deshaies for Plx1; and J. Hammer (NHLB, NIH) for pCMV2-FLAG-MC-ST.

27 March 2001; accepted 11 June 2001

Cohesin Cleavage by Separase Required for Anaphase and Cytokinesis in Human Cells

Silke Hauf, Irene C. Waizenegger, Jan-Michael Peters*

Cell division depends on the separation of sister chromatids in anaphase. In yeast, sister separation is initiated by cleavage of cohesin by the protease separase. In vertebrates, most cohesin is removed from chromosome arms by a cleavage-independent mechanism. Only residual amounts of cohesin are cleaved at the onset of anaphase, coinciding with its disappearance from centromeres. We have identified two separase cleavage sites in the human cohesin subunit SCC1 and have conditionally expressed noncleavable SCC1 mutants in human cells. Our results indicate that cohesin cleavage by separase is essential for sister chromatid separation and for the completion of cytokinesis.

In eukaryotes, replicated DNA molecules remain attached to each other until the onset of anaphase. This sister chromatid cohesion depends on a protein complex called cohesin (1). In yeast, sister chromatid separation is initiated by cleavage of cohesin's subunit Scc1p/Mcd1p by the protease separase (2, 3). This reaction removes cohesin from chromosomes and may directly dissolve cohesion between sister chromatids. In metaphase, separase is activated by the anaphase-promoting complex or cyclosome (APC), which mediates the ubiquitin-dependent proteolysis of the separase inhibitor securin (4–9).

In vertebrates, cohesin is removed from chromosomes in two steps. During prophase and prometaphase, the bulk of cohesin dissociates from the arms of condensing chromosomes (10) by a mechanism that depends neither on the APC-separase pathway nor on cleavage of the human ortholog of Scc1p/Mcd1p, SCC1 (11). A small amount of cohesin remains in centromeric regions until metaphase and is removed from chromosomes only at the onset of anaphase (9). In spread chromosomes from HeLa cells arrested in a preanaphase state, the absence of SCC1 staining on chromatid arms correlates

with the lack of arm cohesion (Fig. 1, A and B), supporting the notion that loss of cohesin is required for sister chromatid separation. The disappearance of residual amounts of SCC1 staining from centromeres coincides with the APC- and separase-dependent cleavage of a small amount of SCC1 (9). It is unknown, however, if this cleavage reaction, which affects maximally 10% of the total cellular cohesin, is required for anaphase.

To analyze the role of SCC1 cleavage in human cells, we identified two cleavage sites in SCC1. To map the NH₂-terminal site, we generated a series of in vitro-translated NH₂- and COOH-terminal truncation mutants of SCC1 and compared their electrophoretic mobilities to those of the COOH- and NH₂-terminal in vivo cleavage products, respectively (Fig. 1C). These analyses suggested that amino acid residues 168 to 182 contain the NH₂-terminal cleavage site. Comparison of this region with the recognition site consensus of yeast separase (2, 12, 13) suggested that human SCC1 is cleaved after Arg¹⁷² (Fig. 1D). The analysis of recombinant versions of SCC1 containing small deletions or point mutations in this region confirmed this hypothesis (Fig. 1E). The same strategy was used to identify Arg⁴⁵⁰ as the COOH-terminal SCC1 cleavage site (Fig. 1, D and E) (14). Mutation of both sites abolished SCC1 cleavage by separase in vitro (Fig. 1F). Comparison of these sites with known separase cleavage sites in budding and fission yeast (2,

12, 13) yields glutamate-X-X-arginine as the consensus for the sequence preceding the scissile peptide bond (Fig. 1D). In yeast, Cdc5p kinase mediates phosphorylation of serine residues at the P6 positions preceding the cleavage sites in Scc1p/Mcd1p, which enhances cleavage (15). In the NH₂-terminal cleavage site of human SCC1, this position is occupied by an aspartate residue, suggesting that separase prefers acidic residues at the P6 position.

We generated stable human HeLa cell lines in which physiologic amounts of wild-type or cleavage-site mutants of myc-tagged SCC1 are expressed upon addition of doxycycline (Fig. 2A) (16). Cell lines expressing noncleavable SCC1 proliferated more slowly than did lines expressing the wild-type or single-site mutants (14). Transgene expression was rapidly lost after expression of noncleavable SCC1 (Fig. 2B), indicating that the modified SCC1 interferes with proliferation. All SCC1 mutants were incorporated into 14S cohesin complexes (Fig. 2C) (14) and showed nuclear localization in interphase (Fig. 3H), implying that they acted as functional cohesin subunits. Fluorescence microscopy of mitotic cells (Fig. 2D) and incubation of chromatin fractions in meiotic *Xenopus* egg extracts (Fig. 2E) in which the APC-separase pathway is inactive (11, 17) suggested that the bulk of all SCC1 mutants can be dissociated from chromosomes by the prophase pathway, further demonstrating that this pathway does not depend on SCC1 cleavage. Analysis of SCC1 cleavage in mitotic *Xenopus* extracts using chromatin from the different HeLa cell lines as substrate confirmed that the different SCC1 mutants are noncleavable at either the NH₂- or the COOH-terminal site or at both (Fig. 2F).

Immunofluorescence microscopy suggested that most cells expressing wild-type SCC1 completed mitosis and cytokinesis normally (Fig. 3A), whereas multiple mitotic abnormalities were seen in cells expressing noncleavable SCC1 (Fig. 3B). In the latter cells, the cleavage furrow had often begun to ingress although anaphase had not occurred; i.e., the chromosomes remained at the spindle equator. In these cases, the cleavage furrow appeared to constrict the chromosome mass randomly in either a symmetric or an asymmetric manner (Fig. 3B), resembling the cut phenotype in fission yeast mutants defective in anaphase (18). No cyclin B staining could be observed in the human cells attempting

Research Institute of Molecular Pathology (IMP), Dr.-Bohr Gasse 7, A-1030 Vienna, Austria.

*To whom correspondence should be addressed. E-mail: peters@nt.imp.univie.ac.at